Seismic Vulnerability of R.C. Bridges Exposed to Corrosion

Vulnerabilità Sismica di Viadotti Autostradali in C.A. soggetti a degrado

G. Pasqualato[1], P. Crespi[2], M. Zucca[2], N. Longarini[2]

[1] *SINECO S.p.A., Milan, Italy*

[2] *Department of Architecture, Built environment and Construction engineering (ABC), Politecnico di Milano, Milan, Italy*

ABSTRACT: Recently, the engineering interest about the durability of existing reinforced concrete structures has significantly increased as confirmed by the conspicuous scientific literature. The results of these studies are influencing the development of new structural codes. Among the wide range of existing reinforced concrete structures, motorway viaducts stand out for their strategic relevance. Most of these structures were built between ’60 and ’70 years and, nowadays, the materials degradation phenomena are leading to strength capacity reduction, either in serviceability condition or in presence of exceptional loads such as the seismic action. In order to evaluate the degradation phenomena effects on the seismic vulnerability of motorway viaducts, this paper shows a new procedure to evaluate the seismic performance of reinforced concrete bridges starting from the modelling of the materials degradation - according to several scenarios - and by carrying out multimodal pushover analyses.
The degradation is considered in terms of reduction of the concrete cross-section and steel rebar area. The results give an accurate estimation of seismic performance in terms of seismic vulnerability index variation and consequent management activities (e.g. planning and execution of rehab works). / Durante gli ultimi anni, l’interesse ingegneristico riguardo al tema della durabilità delle opere strutturali realizzate in calcestruzzo armato si è notevolmente accresciuto, come dimostra la letteratura specialistica in questo settore. I risultati di questi studi stanno cominciando a influenzare lo sviluppo dei nuovi codici strutturali. Tra tutte le opere in cemento armato, i viadotti autostradali spiccano per importanza strategica. La maggior parte di questi viadotti è stata realizzata negli anni ’60 e ’70 dello scorso secolo e, oggigiorno, i fenomeni di degrado dei materiali costituenti l’opera stanno portando ad una riduzione della capacità resistente, sia in condizioni di carico di servizio che in presenza di carichi eccezionali come, ad esempio, l’azione sismica. Al fine di valutare l’incidenza dei fenomeni di degrado del calcestruzzo armato sull’incremento della vulnerabilità sismica dei viadotti autostradali, si è provveduto a sviluppare una procedura di verifica che anteponesse alla classica analisi di vulnerabilità sismica, eseguita mediante pushover multimodale, una modellazione del degrado degli elementi del viadotto, in termini di riduzione della sezione di calcestruzzo e d’area delle barre d’armatura longitudinali e trasversali, secondo diversi scenari più o meno severi. Ciò ha consentito di valutare l’evoluzione dell’indice di rischio sismico del viadotto, e del conseguente tempo di intervento, al crescere dell’età dell’opera.

KEYWORDS: seismic vulnerability; bridges; multimodal pushover / vulnerabilità sismica; ponti; pushover multimodale

1 INTRODUCTION

In the last decades, the environmental pollution intensification has led to an increase of the development of corrosion phenomena in reinforced concrete (r.c.) structures.

Among the different forms of concrete structures degradation, one of the most important ones involves the steel rebars corrosion due to external factors as the presence of chlorides in concrete or the carbonation effects.

The durability of reinforced concrete structures has a fundamental influence on their safety evaluation. This is more and more important for strategic structures, like the case of the bridges of the Italian motorway network. In fact, most of these bridges were built in the late 60’s and therefore now they should be subjected to maintenance operations in order to ensure a high safety level. At the same time, awareness and increased attention to seismic capacity evaluation of this type of structures has grown.

This paper investigates the correlation between the carbonation effects on r.c. viaducts and their seismic performance.

2 CORROSION OF STEEL IN CONCRETE: THE CARBONATION EFFECTS

Carbonation occurs when carbon dioxide, from air, penetrates into the concrete and reacts with hydroxides, such as calcium hydroxide, to form carbonates. This chemical reaction reduces the pH value of the

pore solution to as low as 8.5, resulting in a no more stable passive film on the surface of steel rebars.

Two main phases can be identified during the corrosion process development: initiation phase and propagation phase.

Carbonation starts on the external surface of concrete and then propagates toward the inner volume with a parabolic trend characterized by the following penetration law:

$$s = K \cdot t^{1/n} \quad (1)$$

where the thickness of the carbonated layer s advances as a function of the penetration rate coefficient K, through time t. For normal compacted concretes, n is usually assumed equal to 2.

The parameter K, which defines the penetration rate of carbonation, depends on both environmental factors and chemical/physical properties of concrete (Figure 1).

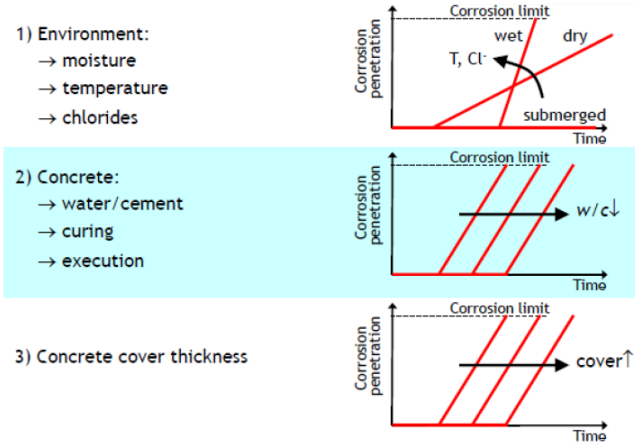

Figure 1. Penetration rate of carbonation / Velocità di penetrazione della carbonatazione

Once the depth of the carbonated layer reaches the concrete cover thickness, the passive layer around rebars is destroyed and steel corrosion begins. In this second phase, the main factor which determines the amount of corrosion rate is the concrete resistivity, while other concrete characteristics such as cement type, water/cement ratio, etc., play a secondary role.

The corrosion rate is negligible for low relative humidity (less than 50%) and only in saturation condition it is possible to reach maximum corrosion rate values near 100 μm/year. Typical corrosion rate values for environmental natural conditions, considering atmospheric agents' interaction effects, range between 5 and 50 μm/year. It is possible to observe that, in the maximum carbonation rate conditions (relative humidity between 50 and 80%), the corrosion is characterized by low penetration rate and vice versa. It is therefore considered that the worst situation is characterized by alternation of low and high humidity conditions, as it happens in the case of concrete exposed to rain.

When the steel rebar corrosion is due to carbonation effects, it is necessary to consider both the initiation t_i and propagation t_p time. By defining a maximum diameter reduction value of the rebars P_{lim} related to the relevant structure limit state (e.g. life safety or operational loss), it is possible to define the following equation:

$$t_{res} = t_i + t_p - t_{actual} = (c/K)^2 + (P_{lim}/i_{corr}) - t_{actual} \quad (2)$$

where: t_{res} is the residual working life of the structure [years], t_{actual} the age of the structure, K the carbonation coefficient [mm/years$^{0.5}$], i_{corr} the mean corrosion rate and c the concrete cover thickness [mm].

To carry out a correct corrosion development analysis, it is necessary to subdivide the structure in homogeneous regions characterized by same concrete cover thickness and environmental exposure conditions.

3 PUSHOVER ANALYSIS

3.1 *Introduction*

The pushover analysis allows the evaluation of nonlinear behavior of structures under an incremental horizontal action. This kind of analysis is widely used in the evaluation of existing structures and infrastructures seismic behavior; three basic concepts can be found in it (ATC-40, 1996): the capacity curve, the demand spectrum and the performance point.

The capacity curve characterizes the resistance capacity of a structure subjected to a horizontal loading profile up to a predefined limit condition. This curve is usually plotted in a diagram correlating the top displacement in relation to the base shear of the whole structure. The increasing horizontal load profile is often assumed as a vibration mode shape:

$$\mathbf{s_n}^* = \mathbf{M\Phi_n} \quad (3)$$

where: $\mathbf{M}$ is the mass matrix of the structure, $\mathbf{\Phi_n}$ is the n-th eigenvector and $\mathbf{s_n}^*$ is the loading vector applied to the structure. The capacity curve can be converted in the so-called ADRS plane, in terms of spectral displacement S_d and spectral acceleration S_e:

$$S_e = V_{bn}/ M_n^* \ , \ S_d = u_{rn}/\Gamma_n\Phi_{rn} \quad (4)$$

where: V_{bn} is the base shear of the structure for the n-th mode shape, u_{rn} is the top displacement value of the monitoring point for the n-th mode shape, M_n^* is the modal mass of the n-th mode, Γ_n is the modal participation factor and Φ_{rn} is the monitoring point component of the n-th eigenvector.

The demand curve of the design earthquake is also represented by an ADRS spectrum, that can be obtained from horizontal acceleration response spectrum by means of the following equation:

$$S_d = (1/4\pi^2) \cdot S_e \cdot T^2 \quad (5)$$

where T is the vibration period of the structure.

The performance point is then defined as the intersection point, in the ADRS plane, between the capacity curve and the demand curve (Fig. 2a), representing the situation in which the structure is actually working under the considered specific seismic input.

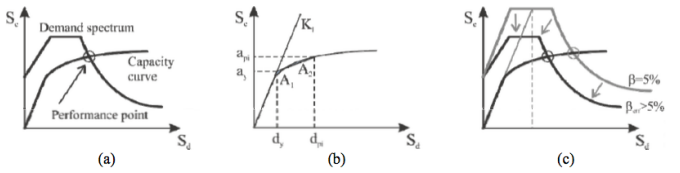

Figure 2. Performance point calculation (a), capacity curve idealization (b), scaled demand spectrum (c) / Calcolo del punto di funzionamento (a), modello idealizzato della curva di capacità (b), spettro di domanda scalato (c)

In order to calculate the performance point, several techniques have been proposed over the years (Causevic and Mitrovic, 2011). A demand reduction coefficient (in terms of behavior factor or damping coefficient) can be calculated through a bi-linearization of the capacity curve (Fig. 2b), in order to take into account the energy dissipation which occur in the post-elastic phase. The intersection between the reduced demand spectrum and capacity curve identifies the performance point related to the specific seismic input. The performance point evaluation method adopted in this work is the Capacity Spectrum Method (CSM) (ATC-40, 1996; FEMA 356, 2000; FEMA 440, 2005). This procedure involves the following main points:

1. seismic demand definition in terms of ADRS spectrum;
2. determination of the first point a_{pi}, d_{pi} on the capacity curve (Fig. 2b);
3. bi-linearization of the capacity curve with a K_I elastic stiffness, followed by a hardening branch having a slope defined by the energy equivalence rule between the capacity curve and its bi-linear idealization. This rule defines the two equal areas A_1 and A_2 and the ideal yielding point a_y and d_y, as well as the first intersection point a_{pi}, d_{pi} (Fig. 2b);
4. scaling of the demand spectrum on the basis of the effective damping coefficient calculated by taking into account both the hysteretic damping (related to the cyclic plastic deformations) and the inherent damping (Fig. 2c);
5. evaluation of the performance point by intersection of the capacity curve and the scaled demand spectrum by means of an iterative procedure.

3.2 *Multi-Modal Pushover Analysis*

In the case of special structures, such as motorway bridges, the choice of the load profile adopted to control pushover analysis is not unique and may decisively influence the results. For this reason, various pushover analysis methods have been proposed to take into account the dynamic behavior of the structure, evaluating the nonlinear seismic response by means of combination of several significant modes (Chopra and Goel, 2002). In this case, N capacity curves must be determined, one for each considered vibration mode. For each considered modal load profile, the relative performance point is calculated considering the relevant seismic demand spectrum. After the evaluation of the performance point, the value of displacements or stresses of the various structural elements, for each mode, are combined by means of the classical modal combination rules: CQC or SRSS.

4 STRUCTURAL MODELLING

4.1 *Introduction*

For the implementation of finite element models of bridge structures, it is possible to use only linear elements in order to limit the computational costs and to obtain results that can be used directly for design considerations.

The stiffness reduction of the structural elements caused by concrete cracking, especially for the piers, is an important aspect to be taken into account in the simulation of the dynamic behavior of bridges. This phenomenon can be considered by applying a specific scaling coefficient to the concrete gross section elastic stiffness, obtained from the moment-curvature (M-χ) diagram, according to Eurocode 8-2 (§ 2.3.6.1, 2005). During the analysis, the sum of structural and nonstructural masses is considered, but the masses of traffic loads are neglected (NTC, § 3.2.4, 2008).

Another fundamental step in the implementation of pushover analysis regards the definition of the material non-linearity. Two different types of resistance mechanisms can be recognized in the behavior of structural elements: a “ductile mechanism”, characterized by load-displacement curves in which an elastic phase is followed by an extended plastic branch and, on the other hand, a “brittle mechanism”, represented by a linear load-displacement relation-ship up to failure, beyond which there is a sudden drop of resistance.

In the case of reinforced concrete bridge piers, the "ductile mechanism" is closely related to the rotational capacity of the plastic hinges. On the contrary, the "brittle mechanism" is controlled by the shear strength of the structural element.

4.2 *Materials*

The choice of material constitutive laws is a critical step in modelling because of its direct influence on the nonlinear analysis results. In particular, constitutive laws must take into account, even if in a simplified way, the complex phenomena that occur inside the structural elements. Concrete behavior is significantly affected by the amount of transverse reinforcement through the confinement effect. The concrete model proposed by Kent and Park is adopted in the following; only the compressive behavior is considered. This constitutive law allows to take into account the effect of transverse reinforcement confinement on the compressive strength by means of the confinement parameter K (Fig. 3a), while the coefficient Z describes the material deterioration in softening phase. The Park strain hardening model is used for steel reinforcement.

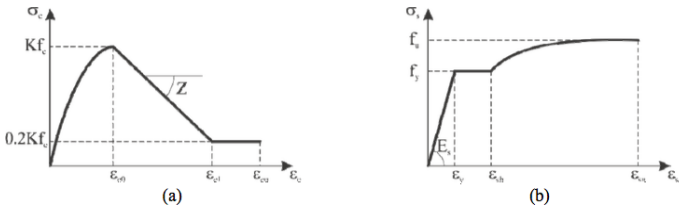

Figure 3. Concrete (a) and steel (b) constitutive laws / Leggi costitutive del calcestruzzo e dell'acciaio

4.3 *Ductile collapse mechanism*

The non-linear behavior of the structure is introduced in the finite element model of the viaduct by means of appropriate plastic hinges, usually placed at the base of the piers (Fig. 4), where the formation of a ductile mechanism can be assumed.

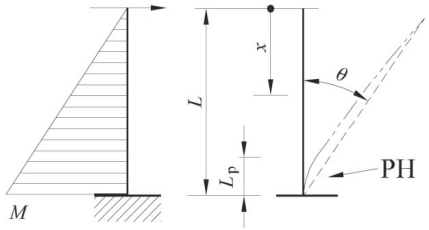

Figure 4. Location and modelling of the plastic hinge (PH) at the base of a pier / Individuazione e modellazione della cerniera plastica alla base delle pile

The needing to define an analytical model of the plastic hinge suggests to extrapolate it from the moment-curvature M-χ curve with the selection of a couple of values that summarize the performances of the section behavior. The first yield point is used to define the stiffness of the cracked section and the load level which corresponds to the beginning of the hardening branch. The second M-χ point is assumed as the ultimate curvature and allows the definition of the ultimate capacity of the member in terms of "curvature ductility" μ_ϑ, defined as the ratio between the ultimate and yield curvatures:

$$\mu_\vartheta = \chi_u / \chi_y \quad (6)$$

After that, the information taken from the M-χ curve have to be transformed in a moment-rotation diagram. This step requires the definition of the plastic hinge length L_{pl}, over which the sectional curvatures will be integrated. Assuming a constant distribution of bending moment in the plastic hinge region, the yield and ultimate rotations can be defined as follows:

$$\vartheta_y = L_{pl} \cdot \chi_y \,, \quad \vartheta_u = L_{pl} \cdot \chi_u \quad (7)$$

The plastic hinge length L_{pl} is evaluated according to the expression proposed by Eurocode 8 (2005):

$$L_{pl} = 0.1L_V \cdot 0.17h \cdot 0.24 \cdot d_{bl} \cdot f_y / f_c^{0.5} \quad (8)$$

where: d_{bl} is the diameter of the longitudinal reinforcement, f_y is the yield stress of the steel rebars and f_c is the compressive strength of the concrete.

The guideline FEMA-356 (§ 2.4.4.3, 2000) shall be used for the definition of the capacity curves of the structure (base shear versus top displacement). According to this guideline, the plastic hinge constitutive law (Fig. 5a) is defined by an initial linear elastic part (AB), followed by a hardening branch (BC). The point C represents the maximum bending moment of the structural element and the corresponding rotation expresses the point over which there is a sudden decrease in resistance (CD). Finally, the residual strength is described by a constant moment branch conventionally assumed equal to 20% of the maximum moment (DE). Beyond the point E, the structural element provides no resistance.

The verification criterion in terms of rotation, which identifies the achievement of the considered limit state (in this case the "Life safety limit state", SLV in the following), is assumed equal to ¾ of the ultimate rotation ϑ_u, corresponding to the point C in Fig. 5a.

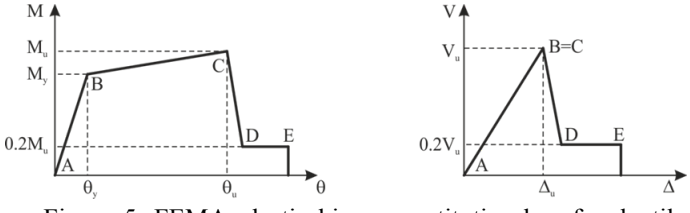

Figure 5. FEMA plastic hinge constitutive law for ductile mechanism (a) and brittle mechanism (b) / Definizione dei le-

gami costitutivi delle cerniere plastiche per il meccanismo duttile (a) e per quello fragile (b) secondo la FEMA

4.4 *Brittle collapse mechanism*

In case of brittle collapse mechanism, the definition of the nonlinear properties must take into account some peculiarities related to the shear behavior of existing reinforced concrete members. These kind of structures were generally designed in the past to resist against small lateral loads. Thus, their horizontal bearing capacity (e.g. seismic resistance) is low.

In the present work, the shear strength of the piers was assumed as reported in Eurocode 8-3 (§ A.3.3.1, 2005), where the cyclic shear resistance V_R in the plastic hinge region is defined as the sum of three factors depending on axial load, concrete strength and transversal rebars.

After the calculation of the shear strength V_R, the analytical elastic-brittle constitutive law proposed in FEMA-356 (2000) is assumed. This curve (Fig. 5b) is based on the same rules previously described for the ductile mechanism except for the absence of a plastic branch, according to the brittle behavior of this kind of failure.

The verification criterion in terms of shear strength, which identifies the achievement of the considered limit state (SLV), is assumed equal to the maximum shear V_R.

5 CASE STUDY

5.1 *Introduction*

In this paper, the above described procedure is applied to a motorway viaduct, as an example. The considered viaduct is characterized by two adjacent and independent carriages, one for each direction, consisting in a sequence of 12 simply supported 32 m length spans (Fig. 6).

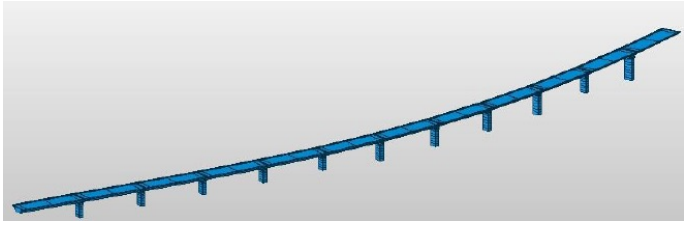

Figure 6. FEM model of the viaduct / Modello ad elementi finiti del viadotto

The viaduct box-girder deck is realized in precast concrete. Each span of the viaduct is supported by 2×3 elastomeric bearings placed at the ends of each longitudinal beam.

Each pier is structurally independent from the adjacent one and it has a hollow rectangular cross section (5.60×2.00 m) and a thickness of 80 cm (Fig. 7). At the top of every reinforced concrete pier, there is a hammerhead cap where the elastomeric bearings are settled. The piers are made of C25/30 cast in place concrete and ALE reinforcing steel.

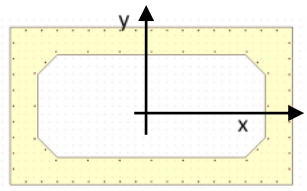

Viaduct - Pier rebars	
Longitudinal	76∅16
Transversal	∅8/15

Figure 7. Piers section / Sezione delle pile

5.2 *Degradation analysis*

The carbonation corrosion effects on rebars, in terms of diameter reduction, are evaluated in three different scenarios characterized by different increasing corrosion. The degradation law adopted in this work is governed by the following equations, regarding bar diameter (d) and cross section area (A_s) respectively:

$$d(t) = d_0 - 2P_x = d_0 - 2i_{corr}k(t - t_i) \quad (9)$$

$$A_s(t) = \pi[d_0 - 2i_{corr}k(t - t_i)]^2 / 4 \quad (10)$$

The rebars diameter reduction ($d_0 - d$) depends on two parameters: the intensity of corrosion i_{corr} and the initiation time t_i. The first parameter is provided by experimental results and design codes while the initiation time has been considered as a statistical variable. Initially, the concrete cover thickness was assumed to be 25 mm. This procedure was repeated assuming different concrete types.

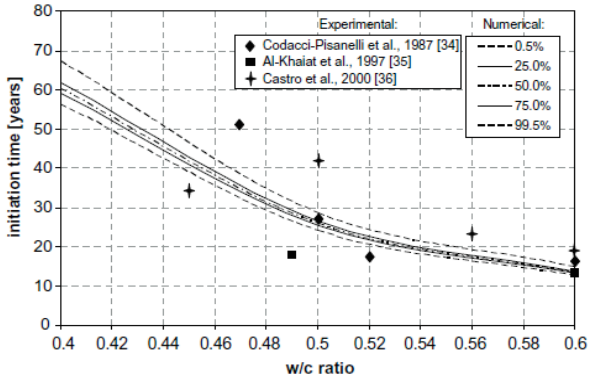

Figure 8. Initiation time vs w/c ratio / Tempo di innesco in relazione al rapporto acqua cemento del calcestruzzo

An initiation time of 13.5 years and a water/cement (w/c) ratio of 0.6 (Tab. 1, Fig. 8) were considered in this work because the viaduct was built between ‘60 and ‘70 years. The corrosion intensity ratios are taken according to EURAM standards (Tab. 2). Three corrosion scenarios are considered: slight, moderate and high corrosion levels.

Table 1. Initiation time estimation / Stima del tempo di innesco

w/c	Probability 99%	50%
0.4	61.7 years	60.4 years
0.5	26.3 years	26.0 years
0.6	13.7 years	13.5 years

Table 2. Corrosion intensity estimation / Stima dell'intensità della corrosione

Corrosion level	Dhir et al.	Brite/EURAM	Middleton et al.
Negligible	-	< 0.1	-
Slight	0.1	0.1÷0.5	0.1÷0.2
Moderate	1.0	0.5÷1.0	0.2÷1.0
High	10	> 1.0	> 1.0

Moreover, degradation effect was evaluated in two different times: at building time and after 45 years of service life. In this way, it is possible to evaluate the seismic vulnerability increase of the viaduct with time. The constant parameters for the three above mentioned scenarios are resumed in Table 3. The following Figure 9 summarizes the evaluation of the progressive diameter reduction of both longitudinal and transversal rebars due to corrosion, calculated through equations (9) and (10).

Table 3. Constant parameters / Parametri costanti

Parameter	Value
f_{ck}	25 MPa
t_i	13.5 years
k	0.0116
t	45 years
$\varepsilon_{u,0}$	9%

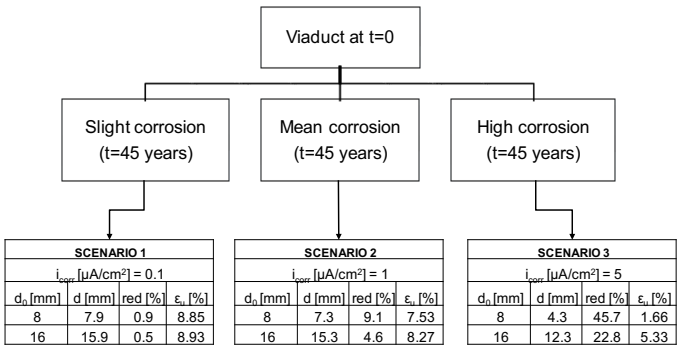

Figure 9. Corrosion flow chart / Diagramma di flusso della corrosione

Even if scenarios 1 (slight) and 3 (high) are not realistic on the basis of the on-site corrosion measurements, their results are here still considered for comparison purposes.

The evolution of the moment-curvature diagrams of the base cross section of piers, for the three different corrosion scenarios, is reported in Figures 10 and 11. Figure 10 shows a decrease in terms of both maximum moment and ductility, when corrosion increases. Differently, in y-y direction (Fig. 11), it is possible to observe a decrease of maximum moment together with an increase of ductility, according to Bossio et al. (2014).

Another consequence of the corrosion process is a progressive reduction of piers stiffness, resulting in an increase of vibration natural periods, especially for the principal modes (Fig. 12).

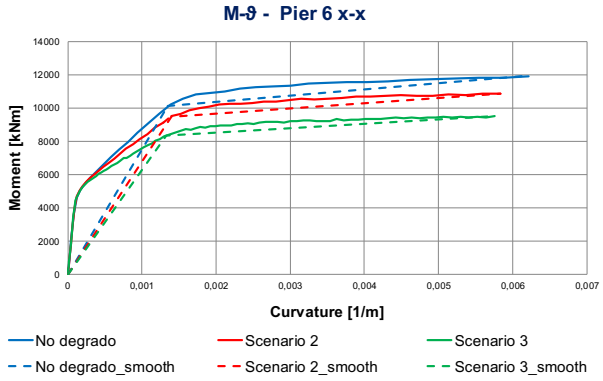

Figure 10. Moment-Curvature diagram (x-x direction) / Diagramma Momento-Curvatura in direzione x-x

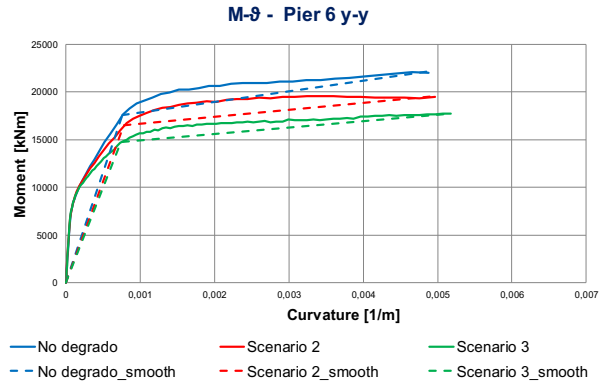

Figure 11. Moment-Curvature diagram (y-y direction) / Diagramma Momento-Curvatura in direzione y-y

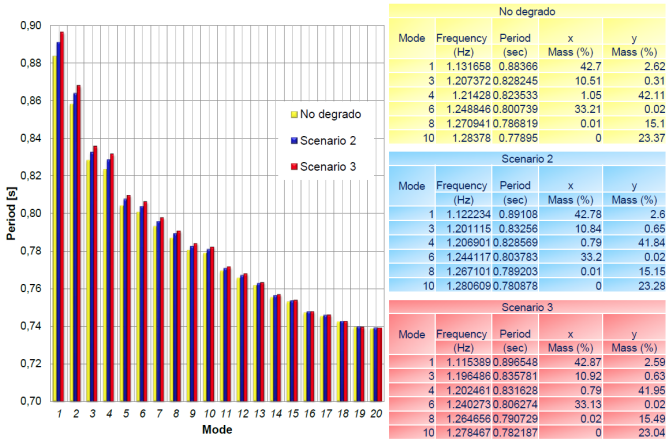

Figure 12. Natural periods for the three different corrosion scenarios / Valore dei periodi per i tre diversi scenari di corrosione

Finally, capacity curve for all the significant vibration modes shapes of the viaduct can be determined according to the procedure described in paragraph 5, for the three scenarios (Fig. 13 and 14).

At last, to complete the vulnerability assessment, the multi-modal pushover analysis con be developed iteratively by increasing the seismic demand spec-

trum, until the required limit state is reached. The seismic demand related to the achievement of a particular limit state can be characterized by its peak ground acceleration $a_{g,max}$ or return period $T_{R,max}$ values, that corresponds to the severity and recurrence of the earthquake, respectively.

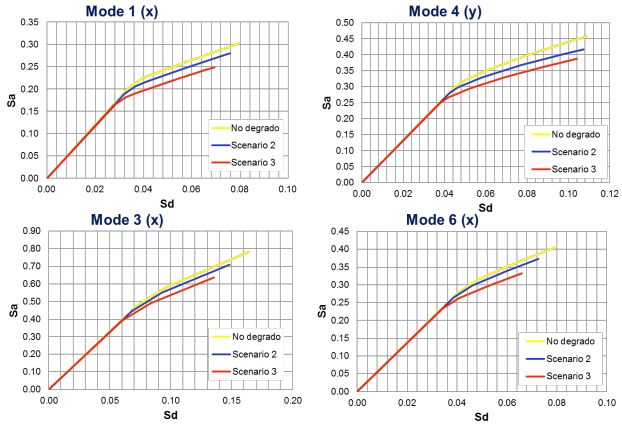

Figure 13. Capacity curves for ductile mechanism / Curve di capacità per il meccanismo duttile

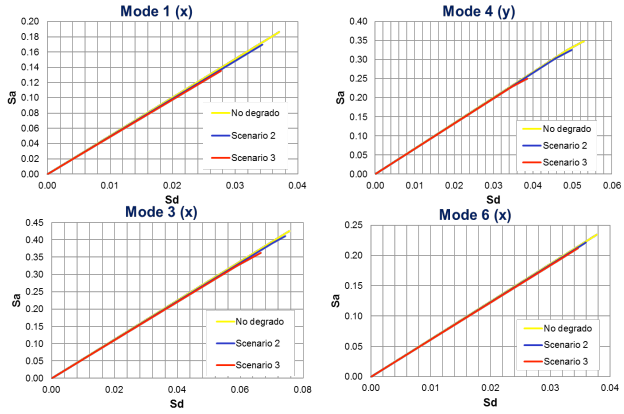

Figure 14. Capacity curves for brittle mechanism / Curve di capacità per il meccanismo fragile

On the basis of these values, the dimensionless risk indices of the viaduct can be calculated as follows:

- risk index in acceleration (IR_{ag}): is the ratio between capacity ($a_{g,max}$) and demand ($a_{g,d}$) in terms of peak ground acceleration (PGA);
- risk index in return period (IR_{TR}): is the ratio between capacity ($T_{R,max}$) and demand ($T_{R,d}$) in terms of return periods of the earthquake.

Values close to one or greater than one characterize cases where the risk level is acceptable; low values close to zero characterize high-risk structures. The risk indices of the considered viaduct are listed in Tables 4 and 5.

Table 4. Risk indices for ductile mechanism / Indici di rischio ottenuti per il meccanismo duttile

	Corrosion level	Ductile Mechanism	
		x	y
IR_{ag}	Undamaged	1.649	2.667
	Moderate	1.552 (-6%)	2.558 (-4%)
	High	1.391 (-16%)	2.387 (-10%)
IR_{TR}	Undamaged	1.931	3.641
	Moderate	1.783 (-8%)	3.446 (-5%)
	High	1.543 (-20%)	3.145 (-14%)

Table 5. Risk indices for brittle mechanism / Indici di rischio ottenuti per il meccanismo fragile

	Corrosion level	Brittle Mechanism	
		x	y
IR_{ag}	Undamaged	0.822	1.327
	Moderate	0.754 (-8%)	1.238 (-7%)
	High	0.619 (-25%)	0.958 (-28%)
IR_{TR}	Undamaged	0.788	1.451
	Moderate	0.714 (-9%)	1.323 (-9%)
	High	0.576 (-27%)	0.949 (-35%)

6 CONCLUSIONS

The over time progressive deterioration of concrete structures implies a reduction of their capacity and a modification of their dynamic behavior under seismic actions.

In this work, the effects of steel corrosion on a reinforced concrete viaduct, caused by carbonation, are analyzed. The degradation was modelled by introducing variations in steel constitutive law and by considering a reduction of rebars area.

The analysis was performed by implementing a viaduct finite element model in three different corrosion scenarios; for each scenario, in order to obtain the values of seismic risk indices, a multi modal pushover analysis was executed. All these models are characterized by concentrated plastic hinges at the base of the piers.

The results showed a general increase of structure vibration periods when degradation increase, together with a loss of resistance for both the ductile and brittle mechanisms (Fig. 15).

Il progressivo deterioramento nel tempo delle strutture in calcestruzzo armato implica una riduzione della loro capacità resistente e una modifica del loro comportamento dinamico in presenza di azioni sismiche.

In questo lavoro sono stati presi in considerazione gli effetti della corrosione indotta dalla carbonatazione. Gli effetti del degrado sono stati modellati introducendo delle variazioni nella legge costitutiva dell'acciaio e considerando una riduzione dei diametri delle barre longitudinali e trasversali.

L'analisi è stata condotta considerando tre differenti scenari di corrosione implementando, per ciascuno di essi, un modello ad elementi finiti. Mediante questi modelli, caratterizzati da cerniere plastiche concentrate alla base delle pile, si sono eseguite delle analisi di tipo pushover multimodale in modo da ottenere gli indici di rischio sismico.

I risultati ottenuti hanno mostrato un aumento del periodo proprio all'aumentare del fenomeno di degrado ed una progressiva perdita di resistenza sia per quanto riguarda il meccanismo duttile sia per quanto riguarda quello fragile.

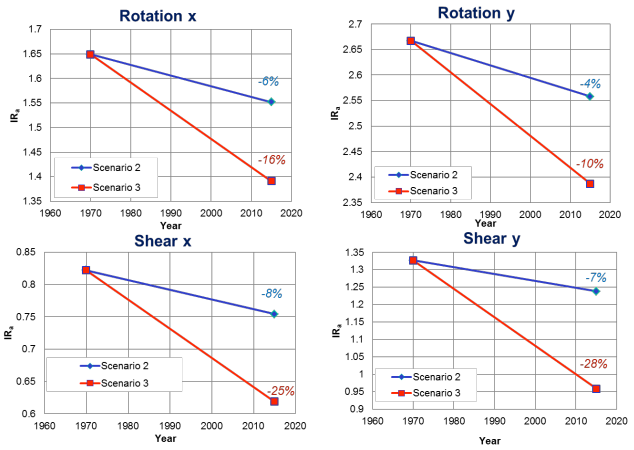

Figure 15. Reduction of risk indices for different scenarios / Riduzione degli indici di rischio per i differenti scenari

ACKNOWLEDGEMENTS

The authors would like to thank SINECO S.p.A. company for the support given to this work. The authors also acknowledge Eng. Alessandro Puccio who worked on this subject during his thesis at Master School F.lli Pesenti of Politecnico di Milano.

REFERENCES

Almusallam, A. 2001. Effect of degree of corrosion on the properties of reinforcing steel bars. *Construction and Building Materials, 15, pp 361-368.*

Andrade, C., Alonso, M.C. & Gonzales, J.A. 1990. An initial effort to use the corrosion rate measurement for estimating rebar durability. *Corrosion rates of steel in concrete, ASTM STP 106, N.S. Berke, V. Chaker and Whinting Eds., American society for testing and materials, pp 29-37: Philadelphia.*

Apostolopoulos, C.A. & Papadakis, V.G. 2008. Consequences of steel corrosion on the ductility properties of reinforcement bars. *Construction and Building Materials, 22, pp 2316-2324.*

ATC-40:1996. Seismic Evaluation and Retrofit of Concrete Buildings, *Applied technology council, 8.1-8.66, Redwood City, CA.*

Berto, L., Saetta, A. & Simioni, P. 2007. Numerical modelling of bond behaviour in RC structures affected by reinforcement corrosion. *University of Padova, Department of Construction and Transportation, IUAV, Department of Architectural Construction.*

Berto, L., Vitaliani, R., Saetta, A. & Simioni, P. 2009. Seismic assessment of existing RC structures affected by degradation phenomena. *University of Padova, Department of Construction and Transportation, IUAV, Department of Architectural Construction.*

Bertolini, L., Elsener, B., Pedeferri, B. & Polder, R. 2004. *Corrosion of steel in concrete. Prevention, diagnosis and repair.* Wiley-VCH, Weinheim.

Bossio, A., Lignola, G.P., Monetta, T., Prota, A., Bellucci, F., Cosenza, E. & Manfredi, G. 2014. Influence of the type of reinforcement on load bearing capacity of corroded reinforced concrete structures. *European Corrosion Congress, Pisa, 8-12 September 2014.*

BRITE/EURAM project 4062:1997. The residual service life of reinforced concrete structures. *Division of Building Materials, LTH, Lund University.*

Cairns, J., Plizzari, G., Du, Y., Law, D. & Franzoni, C. 2005. Mechanical properties of corrosion-damaged reinforcement. *ACI Materials Journal.*

Castel, A., Franfois, G. & Arliguie, G. 2000. Mechanical behaviour of corroded reinforced concrete beams – Part. 1: experimental study of corroded beams. *Laboratoire Mater&iaux et Durabilitè des Constructions (LMDC): Toulouse, France.*

Causevic, M. & Mitrovic, S. 2011. Comparison between nonlinear dynamic and static seismic analysis of structures according to European and US provisions. *Bull. Earthquake Eng., Springer, Vol. 9, No. 2, 467-489.*ATC 40

Chopra, A. K. & Goel, R. K. 2002. A modal pushover procedure to estimate seismic demands of buildings. *Earthquake Engineering and Structural Dynamics, 31:561-582.*

Circolare n. 617 del 2 Febbraio 2009. Istruzioni per l'applicazione delle nuove norme tecniche per le costruzioni di cui al Decreto Ministeriale 14 Gennaio 2008.

Coronelli, D. & Gambarova, P.G. 2004. Structural assessment of corroded reinforced concrete beams: modeling guidelines. *Journal of Structural Engineering.*

Dimitri, V. 2007. Deterioration of strength of RC beams due to corrosion and its influence on beam reliability. *Journal of Structural Engineering.*

Du, Y.G., Clark, L.A. & Chan, A.H.C. 2005. Effect of corrosion on ductility of reinforcing bars. *Magazine of Concrete Research. 57 (7), pp 407-419.*

EN 1998-1:2005. Eurocode 8: Design of structures for earthquake resistance – Part 1: General rules, seismic actions, and rules for building. *CEN (European Committee for Standardization), Management Centre. Brussels.*

EN 1998-2:2005. Eurocode 8: Design of structures for earthquake resistance – Part 2: Bridges. *CEN (European Committee for Standardization), Management Centre. Brussels.*

EN 1998-3:2005. Eurocode 8: Design of structures for earthquake resistance – Part 3: Assessment and retrofitting of buildings. *CEN (European Committee for Standardization), Management Centre. Brussels.*

FEMA 356. Prestandard and commentary for the seismic rehabilitation of buildings. *Federal Emergency Management Agency: Washington, DC.*

FEMA 440. Improvement of nonlinear static seismic analysis procedure. *Applied Technology (ATC-55 Project) Department of Homeland Security, Federal Emergency Management Agency: Washington, DC.*

Franchi, A., Santoro, R., Demofonti, G., Michelis, M., Pipa, M., Gomes, M. & Bianco, L. Optimisation of ductility of welded steel bars, ribbed coils and mesh fabric for reinforced concrete elements under under severe seismic loads. *Final report, EUR EN 20506, Directorate-General for research: Brussels.*

NTCDM 2008. Norme Tecniche per le Costruzioni, 2008.

OPCM 2003, n. 3274. Primi elementi in materia di criteri generali per la classificazione sismica del territorio e normative tecniche per le costruzioni in zona sismica.

UNI 11104:2004. Calcestruzzo – specificazione, prestazione, produzione e conformità – Istruzioni complementari per l'applicazione della EN 206-1.

UNI EN – 206-1:2006. Calcestruzzo – parte 1: specificazione, prestazione, produzione e conformità.